Experimental Evidence for Self-Generated Magnetic Fields and Remote Energy Deposition in Laser-Irradiated Targets

M. A. Yates, D. B. van Hulsteyn, H. Rutkowski, G. Kyrala, and J. U. Brackbill
Los Alamos National Laboratory, Los Alamos, New Mexico 87545

(Received 1 July 1982)

In a series of experiments using two-, four-, and eight-beam 10.6-μm-laser irradiation of a variety of target geometries, a significant amount of energy was found to be deposited in regions remote from the focal spots. The deposition patterns can be predicted with a self-generated magnetic field model.

PACS numbers: 52.50.Jm

Lateral transport of energy away from laser focal spots can play an important role in redistributing energy deposition in laser-fusion targets. Work has been reported investigating the qualitative[1] and quantitative[2] nature of this transport. Recently, using a plasma simulation, Forslund and Brackbill[3] have identified convective transport of electrons in self-generated magnetic fields as an important mechanism for surface transport in laser-irradiated foils. In one simulation with a laser intensity of 5×10^{13} W/cm^2 in a 60-μm spot and a hot-electron temperature of 20 keV, peak fields of the order of 1 MG were calculated. The calculation has not been performed at higher intensities comparable to those used in experiment ($\sim10^{16}$ W/cm^2) because the code does not handle the relativistic effects of the high-energy electrons generated at these intensities. In general, the ratio of electron to magnetic field pressure is of order 1 in a magnetized sheath whose thickness is large compared with the electron gyroradius. This Letter presents experimental evidence for the nonuniformity of energy deposition predicted by the magnetic field model in a variety of target geometries progressing from flats to cylinders to spheres.

From the simulations, a simple qualitative model has been developed. Briefly, the model describes lateral energy transport by electrons in magnetic fields generated at the periphery of the laser spot by lateral temperature gradients in the corona. These gradients are maintained by electrons confined and drifting in the magnetic field, resulting in the convective transport of energy from the beam spot to the edge of the magnetized region. The interaction of the magnetic field and electrons produces a thermal magnetic wave[4] which propagates across the surface until disrupted by fringing fields at the target edge or by destructive interference with the wave propagating from an adjacent beam.

A result of this description is that the higher-energy electrons which transport energy away from the laser spot are magnetically insulated from the target surface. However, where thermal magnetic waves from adjacent beams interfere, as depicted in Fig. 1(a), there is a magnetic field null. At that point the electrons deposit their energy into the target. We have performed an experiment with two beams on a flat target which dramatically shows this effect, as seen in Fig. 1(b). In addition, we have taken data in more complex geometries which also show patterns of deposition consistent with transport dominated by self-generated fields.

All experiments were performed at the Helios laser facility[5] of the Los Alamos National Laboratory. This is a carbon-dioxide system with a

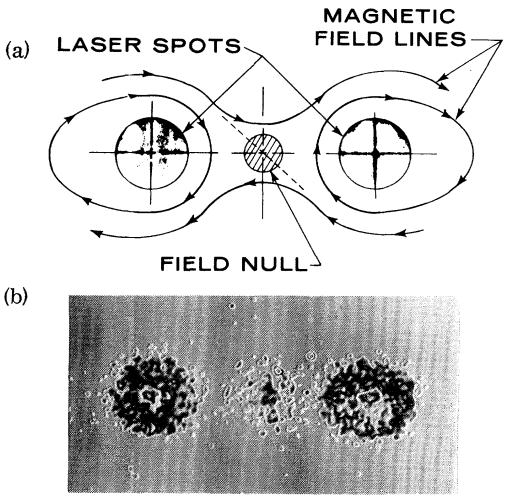

FIG. 1. Energy deposition region between two laser beams as (a) predicted by simulations using convective electron transport in self-generated magnetic fields and (b) recorded experimentally with an x-ray pinhole camera from two beams spaced 1 mm apart on a flat gold target.

wavelength of 10.6 μm and a skewed Gaussian pulse shape with a rise time of 200 ps, decay time of 1600 ps, and full width at half maximum of 650 ps. The average energy used per beam was 700 J into an average focal spot diameter, encircling 86% of the energy, of 120 μm. At this tight focus condition the beams are four times diffraction limited showing no evidence of hot spots. This condition gave an average intensity of $\sim 10^{16}$ W/cm^2. The temperature of the hot electrons created at this intensity was measured via bremsstrahlung to be ~ 200 keV. The data shown in Figs. 1–4 are x-ray pinhole photographs which show the time-integrated energy deposition in six variations of irradiation and target configuration. The targets in Figs. 1(b) and 4 were gold; those in Figs. 2 and 3(b) were nickel; and that in Fig. 3(a) was copper. The single images were taken with 25-μm pinholes filtered with 8.5 μm of beryllium allowing through all x rays above ~ 1 keV. The triple images were taken with a three-aperture (each 100 μm) pinhole camera filtered with 22.5 μm Co, 8.5 μm Be, and 20 μm Ni, respectively. The cobalt and nickel filters were matched so that subtracting their images would give the K_α image for the copper targets. Most of the signal comes from the high-energy continuum. The film used was either Kodak SB-5 or 103-AG, which is most responsive to x rays in the region of 1–10 keV.

The targets used in the two-beam experiment were 9-mm-diam, 25-μm-thick gold disks. The focal spots in this shot [Fig. 1(b)] were separated by 1 mm. The observed deposition region corresponds to the interference pattern predicted by the lateral transport model when two beams are turned on simultaneously. When one beam is delayed by 100 ps, the central deposition region is not observed. We believe this indicates that the magnetic field from one spot has spread beyond the second spot before the second field is turned on, eliminating the region of magnetic field null. This implies that the velocity of the thermal magnetic wave is $>1\times10^9$ cm/s in agreement with measurements of lateral speed made by Jaanimagi *et al.*,[1] and with the calculations.[3]

The next set of flat targets were 1 mm $\times$ 4 mm rectangular foils, 25 μm thick, irradiated from one side with four beams focused along the foil with separation between beam spots of 1 mm. The data in Fig. 2(a) show distinct deposition tracks halfway between the focal spots and along the edges with rings of little or no deposition adjacent to the focal spots. When this target is curved to form a 500-μm-diam cylinder and irradiated by four beams evenly spaced around the surface, the spiral pattern in Fig. 2(b) results. Again energy is deposited only at focal spots, along edges, and at interference regions between beams.

The targets in Fig. 3 are 500-μm- and 250-μm-diam wires, respectively, with all eight beams of Helios arrayed as four pairs along the wire at 1-mm spacings. Here the areas adjacent to the fo-

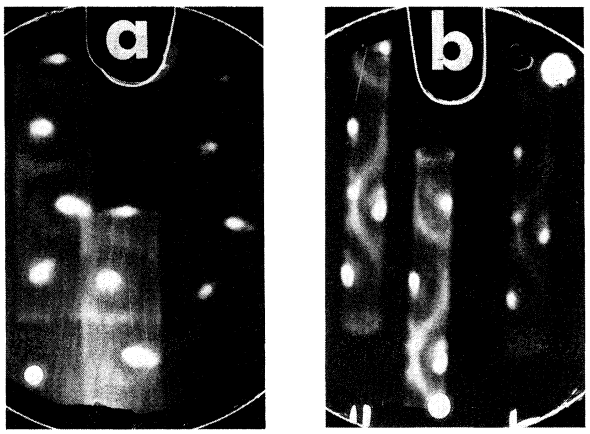

FIG. 2. Triple-aperture (each 100 μm) filtered x-ray pinhole photographs of energy deposition on 25-μm-thick nickel targets irradiated with four beams at 1-mm spacing on (a) a flat and (b) a cylinder. The filters used were 22.5 μm Co, 8.5 μm Be, and 20 μm Ni, as seen left to right.

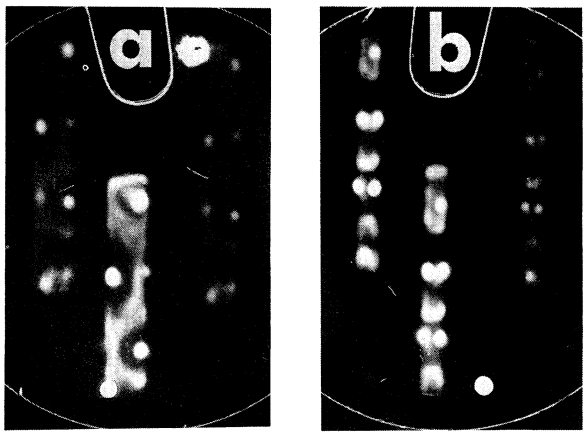

FIG. 3. Triple-aperture (each 100 μm) filtered x-ray pinhole photographs showing (a) a spiral pattern on a 500-μm-diam copper wire and (b) a ring pattern on a 250-μm-diam nickel wire when irradiated with four pairs of opposing beams at 1-mm spacings. The filters were 22.5 μm Co, 8.5 μm Be, and 20 μm Ni, as seen left to right.

FIG. 4. X-ray pinhole photograph of energy deposition in a 300-μm-diam gold sphere irradiated symmetrically with eight beams.

cal spots show more plainly little or no deposition but the pattern of deposition (i.e., the shape and limits of the fields) varies with the size of the target or, equivalently, the separation of the beams. While the larger wire still shows the spiral pattern, the deposition regions and the null areas on the smaller wire are in the form of rings around the surface between the pairs of beams. From this, one can see that changing the target shape or the pattern of illumination affects the region of deposition and insulation. Of course, uniform illumination would result in uniform deposition since the fields would have no place to form or transport.

Figure 4 shows the deposition regions observed on a sphere similar to earlier data,[6] again showing tracks between the beams consistent with the magnetic field model. While quantitative analysis of these data is difficult, we estimate by integrating the film density that as much as two-thirds of the deposited energy is in areas remote from the focal spots. Other data on flat targets[2] suggest that as much as 85% of the energy is transported away from the focal spot. The calculations indicate a loss of ~30% to lateral transport, but because a low-intensity linear source was used, this is believed to be an underestimate.

In summary, we have observed that energy deposition by high-energy electrons in targets irradiated by tightly focused lasers is spatially very nonuniform in a way which cannot be produced by flux-limited diffusive transport. The pattern of deposition can be described by using convective electron transport in self-generated magnetic fields. Quantitative studies of the surface insulation and remote deposition are underway to determine if these effects might be useful in designing an efficient laser-fusion target and to allow better interpretation of past data.

We wish to thank the operations, target fabrication, and diagnostics crews whose generous cooperation so aided the completion of these experiments. This work was performed under the auspices of the U. S. Department of Energy.

[1]P. A. Jaanimagi, N. A. Ebrahim, N. H. Burnett, and C. Joshi, Appl. Phys. Lett. 38, 734 (1981); A. W. Ehler, F. Begay, T. H. Tan, and P. H. Castine, J. Phys. 13, L65 (1980); J. C. Kieffer *et al.*, Phys. Rev. Lett. 44, 1128 (1980); R. Decoste, J. C. Kieffer, and H. Pepin, Phys. Rev. Lett. 47, 35 (1981); N. A. Ebrahim *et al.*, Phys. Rev. Lett. 43, 1995 (1979).

[2]F. Amiranoff *et al.*, Max-Planck-Institut fur Quantenoptik Report No. MPQ60, 1982 (unpublished); M. A. Yates, D. B. van Hulsteyn, K. B. Mitchell, and E. Stover, to be published.

[3]D. W. Forslund and J. U. Brackbill, Phys. Rev. Lett. 48, 1614 (1982).

[4]G. J. Pert, J. Plasma Phys. 18, 227 (1977).

[5]R. Carlson *et al.*, IEEE J. Quantum Electron. 17, 1662 (1981).

[6]P. Lee, D. B. van Hulsteyn, A. Hauer, and S. Whitehill, Opt. Lett. 6, 196 (1981).

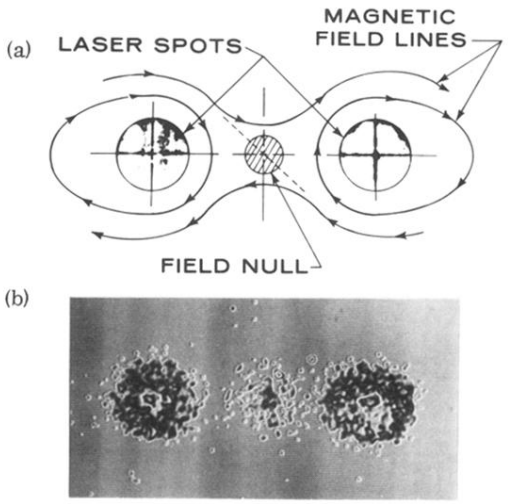

FIG. 1. Energy deposition region between two laser beams as (a) predicted by simulations using convective electron transport in self-generated magnetic fields and (b) recorded experimentally with an x-ray pinhole camera from two beams spaced 1 mm apart on a flat gold target.

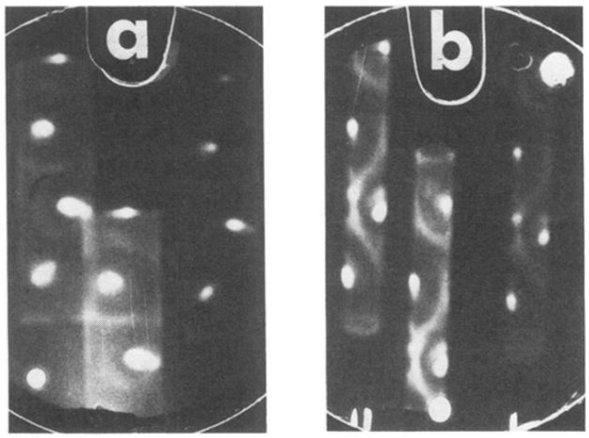

FIG. 2. Triple-aperture (each 100 μm) filtered x-ray pinhole photographs of energy deposition on 25-μm-thick nickel targets irradiated with four beams at 1-mm spacing on (a) a flat and (b) a cylinder. The filters used were 22.5 μm Co, 8.5 μm Be, and 20 μm Ni, as seen left to right.

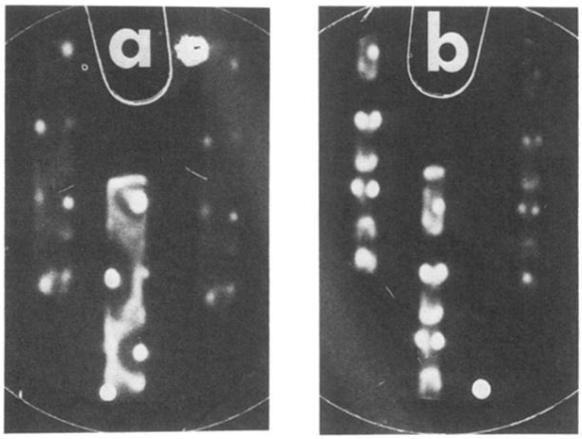

FIG. 3. Triple-aperture (each 100 μm) filtered x-ray pinhole photographs showing (a) a spiral pattern on a 500-μm-diam copper wire and (b) a ring pattern on a 250-μm-diam nickel wire when irradiated with four pairs of opposing beams at 1-mm spacings. The filters were 22.5 μm Co, 8.5 μm Be, and 20 μm Ni, as seen left to right.

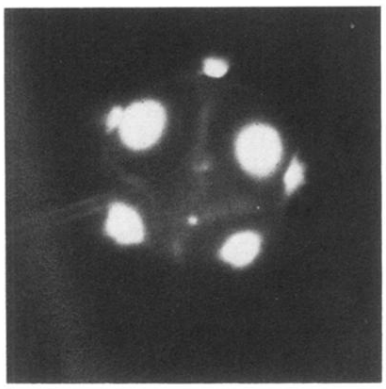

FIG. 4. X-ray pinhole photograph of energy deposition in a 300-μm-diam gold sphere irradiated symmetrically with eight beams.